X-duplex Relaying: Adaptive Antenna Configuration

Shuai Li*, Mingxin Zhou*, Jianjun Wu*, Lingyang Song*,

Yonghui Li†, and Hongbin Li*

* School of Electronics Engineering and Computer Science,
Peking University, Beijing, China
(E-mail: shuai.li.victor, mingxin.zhou, just, lingyang.song, lihb@pku.edu.cn)

†School of Electrical and Information Engineering,
The University of Sydney, Australia
(E-mail: yonghui.li@sydney.edu.au)

arXiv:1701.07168v1 [cs.IT] 25 Jan 2017

Abstract

In this letter, we propose a joint transmission mode and transmit/receive (Tx/Rx) antenna configuration scheme referred to as X-duplex in the relay network with one source, one amplify-and-forward (AF) relay and one destination. The relay is equipped with two antennas, each of which is capable of reception and transmission. In the proposed scheme, the relay adaptively selects its Tx and Rx antenna, operating in either full-duplex (FD) or half-duplex (HD) mode. The proposed scheme is based on minimizing the symbol error rate (SER) of the relay system. The asymptotic expressions of the cumulative distribution function (CDF) for the end-to-end signal to interference plus noise ratio (SINR), average SER and diversity order are derived and validated by simulations. Results show that the X-duplex scheme achieves additional spatial diversity, significantly reduces the performance floor at high SNR and improves the system performance.

I. Introduction

Deployment of full-duplex (FD) into relay networks is a promising technology to increase the spectral efficiency of wireless relay networks [1]. The FD relays can receive and transmit the signal simultaneously over the same frequency which is contrary to the half-duplex (HD) relay systems requiring two orthogonal channels. However, the performance of FD relaying is limited by self interference due to the signal leakage at the FD relay node. Various approaches, including antenna isolation [2], analog cancellation [3], have been developed to mitigate the self interference and improve the performance of FD relay systems.

Adaptive mode selection between FD and HD is an effective way to further improve the system performance. The hybrid FD/HD relaying has been investigated and shown that it can effectively improve spectral efficiency [4]. The outage probability performance of an optimal relay selection scheme with hybrid relaying has been analyzed [5]. A joint relay and antenna selection scheme (RAMS) has been proposed

and considerably improved the system performance [6]. The antenna switching has been introduced into the full-duplex wiretap channel to enhance physical layer security and obtain the full secrecy diversity order [8]. When the antennas at relay can be adaptively configured for transmission or reception, there are four possible transmission modes including two HD and two FD modes, as depicted in Fig. 1. Due to the multi-path transmission of the signal leaked from the transmit antenna to the receive antenna at FD node, the residual self interference (RSI) can be modeled as Rayleigh distribution with effective self interference cancellation as [5]–[7]. In this case, the analysis becomes non-trivial.

In this letter, we consider a relay system which consists of one source, one destination and one amplify-and-forward (AF) relay. Given antennas capable of transmission or reception, the relay can dynamically operate in four modes as shown in Fig. 1. We propose to configure the antennas based on minimizing the symbol error rate (SER) of the system. The asymptotic cumulative distribution function (CDF) of the end-to-end signal to interference plus noise ratio (SINR) at the destination is derived. Based on the CDF, the asymptotic average SER and diversity order are derived and validated by numerical simulations. Results show that the X-duplex scheme achieves additional spatial diversity, significantly reduces the performance floor at high SNR and improves the system performance.

II. System Model

In this paper, we consider a two-hop relay system with one source node (S), one AF relay node (R) and one destination node (D), as shown in Fig. 1. The source S transmits the information to the destination D with the help of the relay R, and all nodes operate at the same frequency. The relay R is equipped with two antennas, denoted by A and B, where each antenna is able to transmit/receive the signal. Based on the instantaneous channel state information (CSI) and RSI, the relay adaptively chooses which antenna to transmit/receive to optimize the system performance. For simplicity and without loss of generality, we assume that Tx and Rx antenna at relay remain unchanged in one time slot.

This system can operate in four modes, FD mode A, HD mode A, FD mode B and HD mode B. In FD mode A, relay R set antenna A as Rx antenna and antenna B as Tx antenna. Relay R operates at FD mode, i.e., antenna A receives and antenna B transmits signal simultaneously in one time slot. In HD mode A, the Tx/Rx antenna is the same and relay R operates at HD mode: source S transmits the signal to relay in the first half of one time slot and relay forwards the signal to destination D in the second half of one time slot. In FD/HD mode B, the Tx/Rx antenna at relay is swapped compared with FD/HD mode A.

The channels between the source and relay are denoted as h_1, h_2 and the channels between the relay and destination are denoted as h_3, h_4. The RSI channel from antenna B to antenna A is denoted as h_{SI}^1, and the RSI channel from antenna A to antenna B as h_{SI}^2. All the channels are assumed to follow block Rayleigh fading, where each channel remains unchanged in one time slot and varies from one slot to another

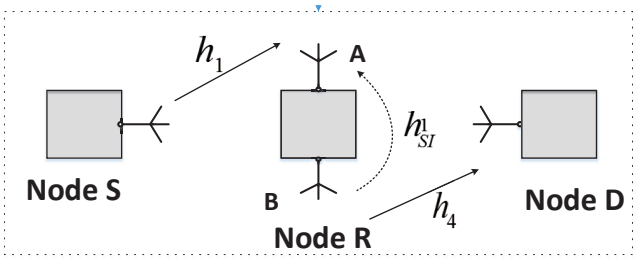

(a) FD mode A

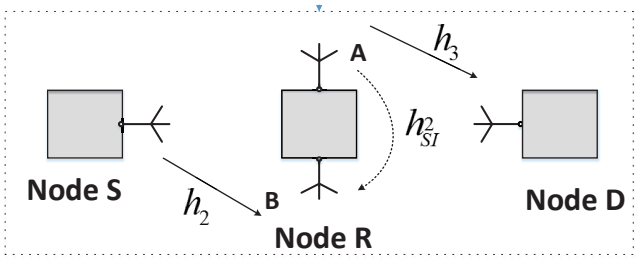

(b) FD mode B

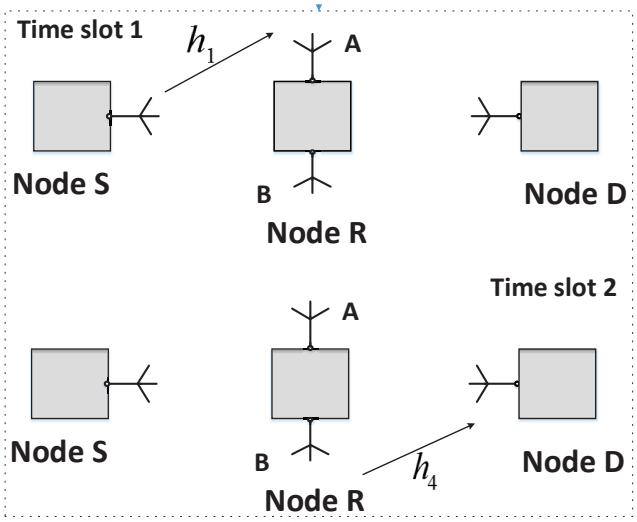

(c) HD mode A

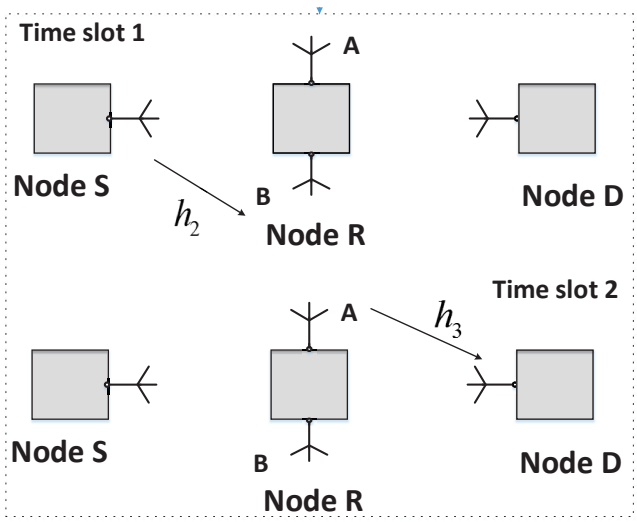

(d) HD mode B

Fig. 1: System model

independently [5]–[7]. The SINR of each mode can be expressed as

$$\begin{aligned} \gamma_{fd_a} &= \frac{X_1 P_R \gamma_4}{X_1 + P_R \gamma_4 + 1}, \gamma_{hd_a} = \frac{P_S P_R \gamma_1 \gamma_4}{P_S \gamma_1 + P_R \gamma_4 + 1}, \\ \gamma_{fd_b} &= \frac{X_2 P_R \gamma_3}{X_2 + P_R \gamma_3 + 1}, \gamma_{hd_b} = \frac{P_S P_R \gamma_2 \gamma_3}{P_S \gamma_2 + P_R \gamma_3 + 1}, \end{aligned} \tag{1}$$

where P_S and P_R are the transmit power of the source and relay. n_R is the additive white Gaussian noise (AWGN) with variance σ^2. $\gamma_i = |h_i|^2/\sigma^2, i \in \{1,2,3,4\}$, ${\gamma^j}_{SI} = |h_{SI}^j|^2/\sigma^2, j \in \{1,2\}$, $X_1 = \frac{P_S \gamma_1}{P_R {\gamma^1}_{SI}+1}$, $X_2 = \frac{P_S \gamma_2}{P_R {\gamma^2}_{SI}+1}$. The channel gain γ_i is modeled as exponential distribution with average mean λ_i and SNR ${\gamma^j}_{SI}$ follows Rayleigh distribution with average mean λ_R^j. In this paper, we assume the two RSI channels identical due to the same self interference cancellation module in two FD modes, $\lambda_R^1 = \lambda_R^2$. The CSIs of h_i and h_{SI}^j can be measured by standard pilot-based channel estimation and sufficient training, and transmitted to the decision node through reliable feedback channels [4], [5]. We assume perfect CSI in this paper.

To optimize the system performance, the X-Duplex can be reduced to one of the four modes with different antenna mode configurations. The average SER with link SINR γ can be written as $\overline{SER} = a_1 \mathbb{E}[Q(\sqrt{2a_2\gamma})]$

[9]. The optimal Tx/Rx mode and duplex mode is determined based on the minimal SER criterion.

$$mode = \arg\min\left\{\overline{SER}\right\} = \arg\max\left\{\tilde{\gamma}_{fd_a}, \tilde{\gamma}_{fd_b}, \tilde{\gamma}_{hd_a}, \tilde{\gamma}_{hd_b}\right\}, \tag{2}$$

where $\tilde{\gamma}$ is the end-to-end SINR of each mode. As the equivalent end-to-end SINR of HD mode can be written as $\tilde{\gamma} = \sqrt{\gamma + 1} - 1$ [4], the SINR of the X-Duplex relay system can be given as

$$\gamma_{\max} = \max\{\gamma_{fd_a}, \gamma_{fd_b}, \sqrt{\gamma_{hd_a} + 1} - 1, \sqrt{\gamma_{hd_b} + 1} - 1\}. \tag{3}$$

III. Performance Analysis

In this section, we derive the CDF of the X-duplex relay system and analyze the system performance, including the average SER and diversity order.

A. Average SER Analysis

The average SER with link SINR γ can be computed as [9]

$$\overline{SER} = a_1 \mathbb{E}[Q(\sqrt{2a_2\gamma})] = \frac{a_1\sqrt{a_2}}{2\sqrt{\pi}} \int_0^\infty \frac{e^{-a_2\gamma}}{\sqrt{\gamma}} F_\gamma(\gamma) d\gamma, \tag{4}$$

where $F_\gamma(\cdot)$ is the CDF of γ, $Q(\cdot)$ is the Gaussian Q-Function [10], (a_1, a_2) denote the modulation formats.

Proposition 1: The asymptotic CDF of the end-to-end SINR of the X-duplex system $\gamma_{\max}$ can be given as

$$\Pr(\gamma_{\max} < x) = (1 - I_1 + I_2) \cdot (1 - I_3 + I_4), \tag{5}$$

$$I_1 = \frac{1}{1+\eta_1 x}\left[\beta_1^1 K_1(\beta_1^1) e^{-C_1 x} + \eta_1 x \beta_2^1 K_1(\beta_2^1) e^{-\beta_3^1}\right],$$
$$I_2 = \frac{2\eta_1(x^2+x)}{\lambda_4 P_R (1+\eta_1 x)^2}\left[K_0(\beta_1^1) e^{-C_1 x} - K_0(\beta_2^1) e^{-\beta_3^1}\right],$$
$$I_3 = \frac{1}{1+\eta_2 x}\left[\beta_1^2 K_1(\beta_1^2) e^{-C_2 x} + \eta_2 x \beta_2^2 K_1(\beta_2^2) e^{-\beta_3^2}\right],$$
$$I_4 = \frac{2\eta_2(x^2+x)}{\lambda_3 P_R (1+\eta_2 x)^2}\left[K_0(\beta_1^2) e^{-C_2 x} - K_0(\beta_2^2) e^{-\beta_3^2}\right],$$

$$\beta_1^1 = 2\sqrt{\frac{x+x^2}{\lambda_1\lambda_4 P_S P_R}}, \beta_3^1 = C_1(x^2+2x) + \frac{x+1}{\eta_1\lambda_1 P_S},$$
$$\beta_1^2 = 2\sqrt{\frac{x+x^2}{\lambda_2\lambda_3 P_S P_R}}, \beta_3^2 = C_2(x^2+2x) + \frac{x+1}{\eta_2\lambda_2 P_S},$$
$$\beta_2^1 = 2\sqrt{\frac{(x^2+2x)^2 + x^2 + 2x + \frac{1}{\eta_1}(x+1)(x^2+2x)}{\lambda_1\lambda_4 P_S P_R}},$$
$$\beta_2^2 = 2\sqrt{\frac{(x^2+2x)^2 + x^2 + 2x + \frac{1}{\eta_2}(x+1)(x^2+2x)}{\lambda_2\lambda_3 P_S P_R}},$$

where $\eta_1 = \frac{\lambda_R^1 P_R}{\lambda_1 P_S}$, $C_1 = \frac{1}{\lambda_1 P_S} + \frac{1}{\lambda_4 P_R}$, $\eta_2 = \frac{\lambda_R^2 P_R}{\lambda_2 P_S}$, $C_2 = \frac{1}{\lambda_2 P_S} + \frac{1}{\lambda_3 P_R}$, $K_1(\cdot)$, $K_0(\cdot)$ are the first and zero order Bessel function of the first and second kind [10].

Proof: The deviation is given in Appendix A. ■

$$\overline{SER} \approx \frac{a_1\sqrt{a_2}}{2\sqrt{\pi}}\left\{\sqrt{\frac{\pi}{a_2}} - \sqrt{\frac{\pi}{\eta_1}}e^{\frac{a_2+C_1}{\eta_1}}\Gamma(\frac{1}{2},\frac{a_2+C_1}{\eta_1}) - \sqrt{\frac{\pi}{\eta_2}}e^{\frac{a_2+C_2}{\eta_2}}\Gamma(\frac{1}{2},\frac{a_2+C_2}{\eta_2}) + \frac{\sqrt{\pi}}{\eta_1-\eta_2}\mathcal{F}^3 - \eta_1 e^{-\frac{1}{\lambda_1 P_S \eta_1}}\mathcal{F}(\frac{3}{2},C_1,\mu_1,\eta_1)\right.$$
$$\left. -\eta_2 e^{-\frac{1}{\lambda_2 P_S \eta_2}}\mathcal{F}(\frac{3}{2},C_2,\mu_1^2,\eta_2) + \frac{\eta_1 e^{-\frac{1}{\lambda_1 P_S \eta_1}}}{\eta_1-\eta_2}\mathcal{F}^2(\frac{3}{2},C_1,\mu_2) + \frac{\eta_2 e^{-\frac{1}{\lambda_2 P_S \eta_2}}}{\eta_1-\eta_2}\mathcal{F}^2(\frac{3}{2},C_2,\mu_2^2) + \frac{\eta_1\eta_2 e^{-\frac{1}{\lambda_1 P_S \eta_1}-\frac{1}{\lambda_2 P_S \eta_2}}}{\eta_1-\eta_2}\mathcal{F}^2(\frac{5}{2},C_2,\mu_3)\right\}, \tag{6}$$

$$\mathcal{F}(v,\beta,\gamma,t) = (2\beta)^{-\frac{v}{2}}\Gamma(v)\, D_{-v}(\frac{\gamma+t}{\sqrt{2\beta}})e^{\frac{(\gamma+t)^2}{8\beta}} - \frac{1}{2}t^2(2\beta)^{-\frac{v}{2}-1}\Gamma(v+2)D_{-v-2}(\frac{\gamma+\frac{5}{3}t}{\sqrt{2\beta}})e^{\frac{(\gamma+\frac{5}{3}t)^2}{8\beta}}, \tag{7}$$

Proposition 2: The asymptotic average SER of the X-duplex system $\gamma_{\max}$ is given in (6).

In (6), $\mu_1 = 2C_1 + a_2 + \frac{1}{\lambda_1 P_S \eta_1}$, $\mu_1^2 = 2C_2 + a_2 + \frac{1}{\lambda_2 P_S \eta_2}$, $\mu_2 = \mu_1 + C_2$,$\mu_2^2 = \mu_1^2 + C_1$,$\mu_3 = 2C_1 + 2C_2 + a_2 + \frac{1}{\lambda_1 P_S \eta_1} + \frac{1}{\lambda_2 P_S \eta_2}$, $\mathcal{F}^2(v,\beta,\gamma) = \eta_1\mathcal{F}(v,\beta,\gamma,\eta_1) - \eta_2\mathcal{F}(v,\beta,\gamma,\eta_2)$, $\mathcal{F}^3 = \sqrt{\eta_1}e^{\frac{C_1+C_2}{\eta_1}}\Gamma(\frac{1}{2},\frac{C_1+C_2}{\eta_1}) - \sqrt{\eta_2}e^{\frac{C_1+C_2}{\eta_2}}\Gamma(\frac{1}{2},\frac{C_1+C_2}{\eta_2})$, $\Gamma(\cdot)$ is the Gamma Function, $\Gamma(a,x)$ is the incomplete Gamma Function, $D_p(\cdot)$ is the Parabolic Cylinder Function [10].

Proof: The deviation is given in Appendix B. ■

When SNR goes infinite, the CDF of FD mode A approaches $\Pr(\gamma_{fd_a} < x) = 1 - \frac{1}{1+\eta_1 x}$. With (4) and [10, eq.(3.383.10)], the lower bound of the SER can be obtained as $\overline{SER}_{SNR\to\infty} = \frac{a_1\sqrt{a_2}}{2\sqrt{\pi\eta_1}}e^{\frac{1}{\eta_1}a_2}\Gamma(\frac{3}{2})\Gamma(-\frac{1}{2},\frac{1}{\eta_1}a_2)$. Compared with FD mode, the X-duplex scheme reduces the error floor and achieves lower SER in the high SNR region.

B. Diversity Order Analysis

According to [11, eq.(10.30)], when z comes close to zero, $K_1(z)$ function converges to $\frac{1}{z}$, and the value of $K_0(z)$ is comparatively small. Therefore, at high SNR, the outage probability of X-duplex relay system can be approximated as

$$P_{out}(x) = (1 - \frac{e^{-C_1 x} + \eta_1 x e^{-\beta_3^1}}{1+\eta_1 x}) \cdot (1 - \frac{e^{-C_2 x} + \eta_2 x e^{-\beta_3^2}}{1+\eta_2 x}), \tag{8}$$

when SNR goes infinite, the outage probability of X-duplex relay system comes to zero.

We assume the identical transmit power of source and relay, $P_S = P_R = P_t$ and $\lambda_1 = \lambda_2, \lambda_3 = \lambda_4, \lambda_R^1 = \lambda_R^2$, the finite SNR diversity order of X-duplex system can be derived with $d(\lambda) = -\frac{\partial \ln P_{out}(\lambda)}{\partial \ln \lambda} = -\frac{\lambda}{P_{out}(\lambda)}\frac{\partial P_{out}(\lambda)}{\partial \lambda}$ [6] as

$$d_{XD} \approx \frac{P_t \cdot \partial[2(1+\eta_1 x)M - M^2]/\partial P_t}{(1+\eta_1 x)^2 - 2(1+\eta_1 x)M + M^2}, M = e^{-\frac{2\rho_1}{P_t}} + \eta_1 x e^{-\frac{2\rho_2}{P_t}}, \tag{9}$$

where $C_3 = \frac{1}{\lambda_1} + \frac{1}{\lambda_4}$, $\rho_1 = C_3 x$, $\rho_2 = C_3(x^2+2x) + \frac{x+1}{\eta_1\lambda_1}$. At high SNR, with Taylor's formula $e^{-x} \approx 1 - x + \frac{1}{2}x^2 - \frac{1}{6}x^3 + ...$, we can derive $d_{XD} \approx \frac{1}{P_t}\frac{\frac{1}{P_t}(2{\rho_1}^2 + 2{\eta_1}^2 x^2 {\rho_2}^2 + 4\eta_1 x \rho_1 \rho_2) + o({P_t}^{-2})}{\frac{1}{{P_t}^2}({\rho_1}^2 + {\eta_1}^2 x^2 {\rho_2}^2 + 2\eta_1 x \rho_1 \rho_2) + o({P_t}^{-3})}$. When SNR goes infinite, d_{XD} approaches two.

With (17), (18), (21) and Taylor's formula $e^{-x} \approx 1 - x$, the diversity order of HD mode A, FD mode A and hybrid FD/HD scheme (HY) proposed in [4] can be derived as

$$d_{HD_a} = \frac{1}{P_t} \frac{C_3(x^2+2x) \cdot e^{-C_1(x^2+2x)}}{1 - e^{-C_1(x^2+2x)}} \approx 1 - \frac{C_3(x^2+2x)}{P_t}, \tag{10}$$

$$d_{FD_a} = \frac{1}{P_t} \frac{C_3 \frac{x}{1+\eta_1 x} e^{-C_1 x}}{1 - \frac{1}{1+\eta_1 x} e^{-C_1 x}} \approx \frac{1 - \frac{x}{P_t} C_3}{1 + \frac{P_t \eta_1}{C_3}} \leq 1 - \frac{x}{P_t} C_3, \tag{11}$$

$$d_{HY} \approx 1 - \frac{1}{P_t} \frac{(C_3 x)^2 + \eta_1 x \Big(C_3(x^2+2x) + \frac{x+1}{\eta_1 \lambda_1} \Big)^2}{C_3 x + \eta_1 x C_3(x^2+2x) + \eta_1 x \frac{x+1}{\eta_1 \lambda_1}}. \tag{12}$$

Remark 1. When SNR goes infinite, the diversity order of HD and HY scheme approaches one. Thus, the X-duplex relay achieves nearly double diversity order compared with HD mode and HY scheme at high SNR.

IV. Simulation Results

In this section, we present the performance of the X-duplex relay system. Without loss of generality, we assume equal power allocation $P_S = P_R$, set all channel gains λ_i to one, and $\eta = \eta_1 = \eta_2$. We consider BPSK modulation and set the threshold R_0 as 2 bps/Hz.

Fig. 2 plots the numerical and analytical results of the outage probability and average SER performance of the X-duplex relay system. The performance of pure FD or HD mode, HY [4], and RAMS [6] are plotted for comparison. The simulated outage probability and SER curves tightly match with the expressions in (8), (6). It can be observed that the proposed X-duplex considerably improves system performance and outperforms the other schemes. In the medium SNR, the diversity order of X-duplex is higher than the pure FD or HD mode, and HY scheme. At high SNR, the performance floor in FD mode and RAMS scheme caused by RSI is significantly reduced in the X-duplex scheme. This is because the X-duplex benefits from the HD mode, whose performance is irrelevant to RSI and improves with the increase of transmit power, thus the impact of the performance floor in FD mode on X-duplex relaying system is mitigated with the increase of SNR.

Fig. 3 compares the finite SNR diversity order of the X-duplex scheme with the conventional pure FD and HD mode, RAMS and HY scheme. The diversity order of X-duplex scheme is higher than other schemes and approaches two at high SNR, which is twice that of HD mode or HY scheme with fixed antennas, which is consistent with remark 1. We can observe that the diversity order of FD mode and RAMS scheme increases to the extreme point in medium SNR, where the influence of RSI on the SINR of FD mode is still small and limited. The curve of RAMS approaches that of X-duplex as FD is more likely to be selected in this region. As SNR continually increases, the impact of RSI on the FD mode gets more severe and the diversity order of FD and RAMS gradually decreases. It is shown that the diversity order of FD mode and RAMS decreases to zero at high SNR due to RSI, thus the performance floor exists at high SNR. By

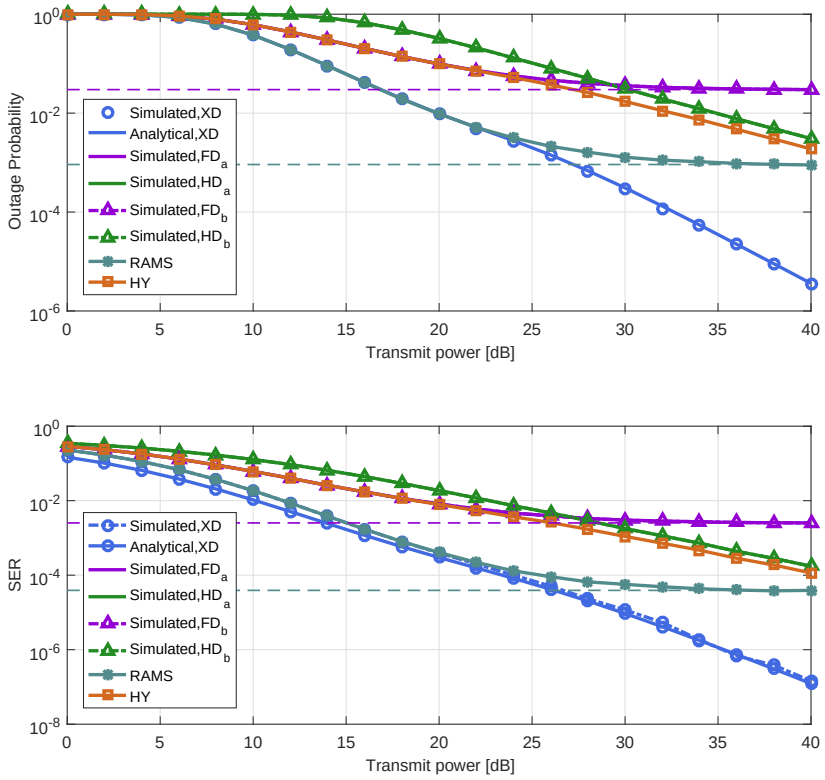

Fig. 2: Outage probability and average SER of X-duplex relay system versus the transmit power when $\eta = 0.01$.

adaptively switching among the four modes, the X-duplex scheme significantly reduces the performance floor and achieves additional spatial diversity.

V. Conclusions

In this letter, we proposed a joint transmission mode and Tx/Rx antenna configuration scheme for the relay network where the relay is equipped with two antennas capable of transmission or reception. In the proposed scheme, the relay adaptively configures its Tx/Rx antenna and duplex mode to minimize the SER. The asymptotic average SER expression and diversity order were derived and validated by simulations. Both analysis and simulations demonstrated that the X-duplex scheme improves the system performance, achieves almost twice diversity order and significantly reduces the performance floor compared to conventional relay schemes.

Appendix A: Proof of Proposition 1

First, the set $\{\gamma_{\max} < x\}$ can be transformed into $\{\gamma_{fd_a} < x, \gamma_{fd_b} < x, \gamma_{hd_a} < x^2 + 2x, \gamma_{hd_b} < x^2 + 2x\}$. As the probability of set $\{\gamma_{fd_a} < x, \gamma_{hd_a} < x^2 + 2x\}$ only contains the probabilities of $\gamma_1, \gamma_4, {\gamma^1}_{SI}$, which

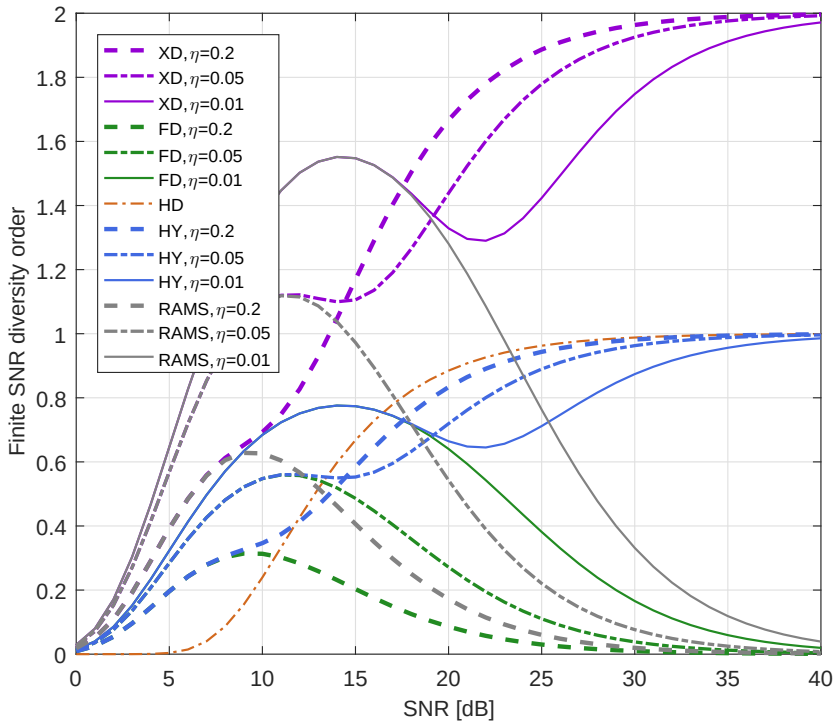

Fig. 3: Finite SNR diversity order versus the link SNR.

are independent from $\gamma_2, \gamma_3, {\gamma^2}_{SI}$ in $\{\gamma_{fd_b} < x, \gamma_{hd_b} < x^2 + 2x\}$. The probability $P^* = \Pr(\gamma_{\max} < x)$ can be further written as

$$P^* = \Pr(\gamma_{fd_a} < x, \gamma_{hd_a} < x^2 + 2x) \cdot \Pr(\gamma_{fd_b} < x, \gamma_{hd_b} < x^2 + 2x). \tag{13}$$

Denoting $P^1 = \Pr(\gamma_{fd_a} < x, \gamma_{hd_a} < x^2 + 2x)$, we can write

$$\begin{aligned} \Pr(\gamma_{fd_a} < x, \gamma_{hd_a} < x^2 + 2x) &= 1 - \Pr(\gamma_{fd_a} > x) \\ &- \Pr(\gamma_{hd_a} > x^2 + 2x) + \Pr(\gamma_{fd_a} > x, \gamma_{hd_a} > x^2 + 2x). \end{aligned} \tag{14}$$

The probability $\Pr(\gamma_{fd_a} > x) = \Pr((X_1 - x)(P_R\gamma_4 - x) > x^2 + x)$ can be derived as

$$\Pr(\gamma_{fd_a} > x) = \frac{1}{\lambda_4} \int_{x/P_R}^{\infty} \frac{e^{-\frac{1}{P_S\lambda_1}(x + \frac{x^2+x}{P_R\gamma_4 - x}) - \frac{1}{\lambda_4}\gamma_4}}{1 + \eta_1(x + \frac{x^2+x}{P_R\gamma_4 - x})} d\gamma_4, \tag{15}$$

at high SNR, we use the following approximation

$$\frac{1}{1 + \eta_1(x + \frac{x^2+x}{P_R\gamma_4 - x})} \approx \frac{1}{1 + \eta_1 x}\left(1 - \frac{\eta_1}{1 + \eta_1 x}\frac{x^2 + x}{P_R\gamma_4 - x}\right), \tag{16}$$

With [10, eq.(3.471.9)], $\Pr(\gamma_{fd_a} > x)$ is obtained. The probabilities $\Pr(\gamma_{hd_a} > x^2 + 2x)$ and $\Pr(\gamma_{fd_a} > x)$ can be derived as

$$\Pr(\gamma_{hd_a} > x^2 + 2x) = \beta_0^1 K_1(\beta_0^1) e^{-C_1(x^2+2x)}, \tag{17}$$

$$\Pr(\gamma_{fd_a} > x) \approx \frac{\beta_1^1 K_1(\beta_1^1)}{1 + \eta_1 x} e^{-C_1 x} - \alpha^1 K_0(\beta_1^1) e^{-C_1 x}, \tag{18}$$

where $\beta_0^1 = 2\sqrt{\frac{(x^2+2x)^2+x^2+2x}{\lambda_1\lambda_4 P_S P_R}}$, $\alpha^1 = \frac{2\eta_1(x^2+x)}{\lambda_4 P_R(1+\eta_1 x)^2}$.

The set $\{\gamma_{fd_a} > x, \gamma_{hd_a} > x^2+2x\}$ can be transformed into $\{\gamma_4 > \frac{x}{P_R}, \gamma_4 > \frac{x^2+2x}{P_R}, \gamma_1 > \frac{P_R\gamma_{SI}^1+1}{P_S}h(\gamma_4), \gamma_1 > \frac{1}{P_S}g(\gamma_4)\}$ where $h(\gamma) = x + \frac{x+x^2}{P_R\gamma - x}$, $g(\gamma) = x^2 + 2x + \frac{(x^2+2x)^2+x^2+2x}{P_R\gamma - x^2 - 2x}$. As the value of $\gamma_{fd_a}, \gamma_{hd_a}$ are positive definite, we only consider the case when $x > 0$. Therefore, the set $\{\gamma_{fd_a} > x, \gamma_{hd_a} > x^2 + 2x\}$ can be further simplified as $\{\gamma_4 > \frac{x^2+2x}{P_R}, \gamma_1 > \frac{P_R\gamma_{SI}^1+1}{P_S}h(\gamma_4), \gamma_1 > \frac{1}{P_S}g(\gamma_4)\}$.

We define $\delta = \frac{1}{P_S}\left[(P_R\gamma_{SI}^1 + 1)h(\gamma_2) - g(\gamma_2)\right]$. when $\delta > 0$, $\gamma_{SI}^1 > \frac{x\gamma_4+\gamma_4}{P_R\gamma_4 - x^2 - 2x}$,when $\delta < 0$, $0 < \gamma_{SI}^1 < \frac{x\gamma_4+\gamma_4}{P_R\gamma_4 - x^2 - 2x}$. Thus, $\Pr\{\gamma_{fd_a} > x, \gamma_{hd_a} > x^2 + 2x\}$ splits into two sub-probabilities, $L_1 = \Pr\{\gamma_4 > \frac{x^2+2x}{P_R}, \gamma_1 > \frac{P_R\gamma_{SI}^1+1}{P_S}h(\gamma_4), \gamma_{SI}^1 > \frac{x\gamma_4+\gamma_4}{P_R\gamma_4 - x^2 - 2x}\}$ and $L_2 = \Pr\{\gamma_4 > \frac{x^2+2x}{P_R}, \gamma_1 > \frac{1}{P_S}g(\gamma_4), 0 < \gamma_{SI}^1 < \frac{x\gamma_4+\gamma_4}{P_R\gamma_4 - x^2 - 2x}\}$. With the approximation in (16), and $\frac{1}{\gamma_4 - x/P_R} \approx \frac{1}{\gamma_4 - (x^2+2x)/P_R}$ at high SNR, [10, eq.(3.324.1)] and [10, eq.(3.462.20)], L_1, L_2 can be derived as

$$L_1 = \frac{\beta_2^1}{1+\eta_1 x}K_1(\beta_2^1)e^{-\beta_3^1} - \alpha^1 K_0(\beta_2^1)e^{-\beta_3^1}, \tag{19}$$

$$L_2 = \beta_0^1 K_1(\beta_0^1)e^{-C_1(x^2+2x)} - \beta_2^1 K_1(\beta_2^1)e^{-\beta_3^1}. \tag{20}$$

With (17), (18), (19), (20), the probability P^1 is given as

$$\begin{aligned} P^1 = 1 &- \frac{1}{1+\eta_1 x}\left[\beta_1^1 K_1(\beta_1^1)e^{-C_1 x} + \eta_1 x\beta_2^1 K_1(\beta_2^1)e^{-\beta_3^1}\right] \\ &+ \frac{2\eta_1(x^2+x)}{\lambda_4 P_R(1+\eta_1 x)^2}\left[K_0(\beta_1^1)e^{-C_1 x} - K_0(\beta_2^1)e^{-\beta_3^1}\right]. \end{aligned} \tag{21}$$

Similarly $P^2 = \Pr(\gamma_{fd_b} < x, \gamma_{hd_b} < x^2 + 2x)$ can be derived. With (13), proposition 1 is proved. Due to the approximations used in (18), (19), the derived CDF (5) is an approximate and asymptotic expression and is quite accurate at high SNR.

Appendix B: Proof of Proposition 2

After substituting (5) into (4) and adopting the approximation in the high SNR region that $K_1(z)$ converges to $\frac{1}{z}$, and that the value of $K_0(z)$ is comparatively small [11, eq.(10.30)], which can be ignored for asymptotic analysis. We can derive

$$\begin{aligned} \overline{SER} \approx \frac{a_1\sqrt{a_2}}{2\sqrt{\pi}}\int_0^\infty \frac{e^{-a_2 x}}{\sqrt{x}}\Bigg\{1 &- \frac{e^{-C_1 x} + \eta_1 x e^{-\beta_3^1}}{1+\eta_1 x} - \frac{e^{-C_2 x} + \eta_2 x e^{-\beta_3^2}}{1+\eta_2 x} \\ &+ \frac{e^{-C_1 x - C_2 x} + \eta_1 x e^{-\beta_3^1 - C_2 x} + \eta_2 x e^{-C_1 x - \beta_3^2} + \eta_1\eta_2 x^2 e^{-\beta_3^1\beta_3^2}}{(1+\eta_1 x)(1+\eta_2 x)}\Bigg\} dx. \end{aligned} \tag{22}$$

With [10, eq.(3.381.4)], $S_1 = \int_0^\infty \frac{e^{-a_2 x}}{\sqrt{x}}dx = {a_2}^{-\frac{1}{2}}\Gamma(\frac{1}{2})$.

With [10, eq.(3.383.10)], $S_2 = \int_0^\infty \frac{e^{-a_2 x - C_1 x}}{\sqrt{x}(1+\eta_1 x)}dx$ is given as

$$S_2 = \frac{1}{\eta_1}\int_0^\infty \frac{e^{-(a_2+C_1)x}}{\sqrt{x}(\frac{1}{\eta_1}+x)}dx = \sqrt{\frac{\pi}{\eta_1}}e^{\frac{1}{\eta_1}(a_2+C_1)}\Gamma(\frac{1}{2}, \frac{a_2+C_1}{\eta_1}). \tag{23}$$

Denoting $S_3 = \int_0^\infty \frac{\eta_1 x \cdot e^{-a_2 x - \beta_3^1}}{\sqrt{x}(1+\eta_1 x)} dx$, when the SNR is high and x is around zero, approximation $\frac{1}{1+x} \approx e^{-x} + \frac{1}{2}x^2 e^{-\frac{5}{3}x}$ [6] is used, with [10, eq.(3.462.1)], S_3 is given as

$$\begin{aligned} S_3 \approx & \int_0^\infty \eta_1 \sqrt{x}(e^{-\eta_1 x} + \frac{1}{2}{\eta_1}^2 x^2 e^{-\frac{5}{3}\eta_1 x}) e^{-a_2 x - \beta_3^1} dx \\ & = \eta_1 e^{-\frac{1}{\lambda_1 P_S \eta_1} + \frac{{\mu_1}^2}{8C_1}} (2C_1)^{-\frac{3}{4}} \Gamma(\frac{3}{2}) D_{-\frac{3}{2}}(\frac{\mu_1}{\sqrt{2C_1}}) \\ & + \frac{1}{2}{\eta_1}^3 e^{-\frac{1}{\lambda_1 P_S \eta_1} + \frac{{\mu_2}^2}{8C_1}} (2C_1)^{-\frac{7}{4}} \Gamma(\frac{7}{2}) D_{-\frac{7}{2}}(\frac{\mu_2}{\sqrt{2C_1}}). \end{aligned} \tag{24}$$

Similarly, $S_4 = \int_0^\infty \frac{e^{-a_2 x}}{\sqrt{x}} \frac{e^{-C_2 x} + \eta_2 x e^{-\beta_3^2}}{1+\eta_2 x} dx$ can be derived. For the last part denoted as S_5 in (22), with some mathematical manipulations, the value can be also derived. Substituting S_1, S_2, S_3, S_4, S_5 into (22), (6) can be obtained. Therefore, proposition 2 is proved.

REFERENCES

[1] J. I. Choi , M. Jain , K. Srinivasan , P. Levis and S. Katti, "Achieving single channel, full duplex wireless communication," in *Proc. 2010 ACM MobiCom*, pp. 1–12, 2010.

[2] T. Riihonen, S. Werner and R. Wichman, "Mitigation of loopback self-Interference in full-duplex MIMO Relays," *IEEE Trans. Signal Process.*, vol. 59, no. 12, pp. 5983–5993, Dec. 2011.

[3] E. Everett, M. Duarte, C. Dick, and A. Sabharwal, "Empowering full-duplex wireless communication by exploiting directional diversity," in *Proc. Asilomar Conf. Signals, Syst. Comput.*, pp. 2002–2006, Nov. 2011.

[4] T. Riihonen, S. Werner and R. Wichman, "Hybrid full-duplex/half-duplex relaying with transmit power adaptation," *IEEE Trans. Wireless Commun.*, vol. 10, no. 9, pp. 3074–3085, Sep. 2011.

[5] I. Krikidis, H. A. Suraweera, P. J. Smith and C. Yuen, "Full-duplex relay selection for amplify-and-forward cooperative networks," *IEEE Trans. Wireless Commun.*, vol. 11, no. 12, pp. 4381–4393, Dec. 2012.

[6] K. Yang, H. Cui, L. Song and Y. Li, "Efficient full-duplex relaying with joint antenna-relay selection and self-interference suppression," *IEEE Trans. Wireless Commun.*, vol. 14, no. 7, pp. 3991–4005, Jul. 2015.

[7] H. A. Suraweera, I. Krikidis, G. Zheng, C. Yuen, and P. J. Smith, "Low-complexity end-to-end performance optimization in MIMO full-duplex relay systems," *IEEE Trans. Wireless Commun.*, vol. 13, pp. 913–927, Feb. 2014.

[8] S. Yan, N. Yang, R. Malaney, and J. Yuan, "Antenna switching for security enhancement in full-duplex wiretap channels," in *Proc. IEEE GlobeCOM TCPLS Workshop.*, pp. 1412–1417, Dec. 2014.

[9] A.J. Goldsmith, *Wireless Communications.* Cambridge University Press, 2005.

[10] D. Zwillinger, *Table of integrals, series, and products,* Elsevier, 2014.

[11] Frank W. J. Olver, Daniel W. Lozier, Ronald F. Boisvert and Charles W. Clark, *NIST Handbook of Mathematical Functions,* Cambridge University Press, 2010.